Volume 8
Number 3
7 February 2024
Pages 413–660

Sustainable Energy & Fuels

Interdisciplinary research for the development of sustainable energy technologies

rsc.li/sustainable-energy

ISSN 2398-4902

ROYAL SOCIETY OF CHEMISTRY

PAPER

Norberto Manfredi *et al.*

Top-ranked efficiency under indoor light of DSSCs enabled by iodide-based DES-like solvent electrolyte

Sustainable Energy & Fuels

ROYAL SOCIETY OF CHEMISTRY

PAPER

View Article Online
View Journal | View Issue

Cite this: *Sustainable Energy Fuels*, 2024, **8**, 504

Top-ranked efficiency under indoor light of DSSCs enabled by iodide-based DES-like solvent electrolyte†

Chiara Liliana Boldrini, [a] Andrea Francesca Quivelli, [a] Filippo Maria Perna, [b] Paolo Biagini, [c] Vito Capriati, [b] Alessandro Abbotto [a] and Norberto Manfredi *[a]

This work presents the next paradigm shift in solar energy technology in which a novel iodide-based DES-like mixture has been first investigated as an active electrolyte solvent in dye-sensitized solar cells (DSSCs) in the absence of any co-solvent and any external iodide source. The optimization of the cell design jointly with a bespoke dye functionalized with a hydrophobic chain, properly positioned along the molecular backbone, ensures (a) one of the highest power conversion efficiencies (PCEs) up to 4% for DSSCs based on non-VOC solvents, and (b) a remarkable temporal stability of nearly 95% over a period longer than 2 months. Higher power conversion efficiency values (up to 8.0%) than those reported in the literature with traditional sensitizers and environmentally friendly electrolytes (*e.g.*, water-based electrolytes) have been achieved under low-light illumination. These results are very promising for the realization of next-generation nature-inspired low-cost and high-performing DSSC devices for indoor and outdoor applications.

Received 24th July 2023
Accepted 4th December 2023

DOI: 10.1039/d3se00949a

rsc.li/sustainable-energy

Introduction

In the present time of increasing demand for energy with net-zero greenhouse gas emissions, growing attention has been paid to the full sustainability of renewable energy sources. Solar energy has experienced a tremendous increase in the energy production share and demonstrated great appeal in the last decades,[1,2] with a variety of different last-generation technologies still increasing their harvesting efficiency.[3] In particular, dye-sensitized solar cells (DSSCs) have attracted much interest since their first appearance in 1991 by Grätzel and O'Regan thanks to their ease of fabrication, their potential low cost, and their versatility.[4] DSSCs are constituted of different components that need to be optimized simultaneously. Thus, much work has been dedicated to the n-type semiconductor (SC), the redox couple, the counter electrode, and the dye-sensitizer.[5–8] DSSCs exhibiting the highest power conversion efficiencies (PCEs) contain a liquid electrolyte solution,[9] typically constituted by the I^-/I_3^- redox pair. This represents a major drawback, since the solvent typically is a volatile organic compound (VOC) that is often flammable and toxic. These characteristics greatly hamper the full sustainability of such devices in any part of their life cycle, from production to the working period and final dismissal. Thus, the replacement of VOCs with alternative eco-friendly media for the electrolyte is highly sought-after. In this vein, different clean alternatives have been proposed throughout the years,[10,11] mostly based on water.[12] This approach leads to a safer electrolyte solution, even if the performance of the cell is lower than that using standard VOCs. Top-ranked water-based DSSCs offer a PCE of *ca.* 4%,[10,13–15] with a single record report of PCE = 7.0%.[16] Most recently, much interest has been focused by the scientific community on DSSCs for application as efficient indoor photovoltaic (PV) devices.[9,10,17–22] Indeed, under low intensity and diffuse illumination, DSSCs have demonstrated a superior efficiency with respect to other technologies, such as silicon-based and organic devices and perovskite solar cells,[23,24] thanks to the possibility of tailoring the absorption properties of the cell using an appropriate dye, which is able to properly match the emission spectrum of the different indoor light sources. At the moment, the current record efficiency reported for VOC-based DSSCs in ambient light is at 38% at 1000 lux.[22]

In addition, safety requirements for a device to be used in an indoor environment are even more pressing than those for outdoor devices. The possibility to replace standard VOCs, which represent a relevant safety risk in the presence of leakages or accidental breakage, with more environmentally

[a]*Department of Materials Science and Solar Energy Research Center MIB-SOLAR, University of Milano-Bicocca, INSTM Milano-Bicocca Research Unit, Via Cozzi 55, I-20125 Milano, Italy. E-mail: norberto.manfredi@unimib.it*

[b]*Dipartimento di Farmacia-Scienze del Farmaco, Università di Bari "Aldo Moro", Consorzio C.I.N.M.P.I.S, Via E. Orabona 4, I-70125, Bari, Italy*

[c]*Renewable, New Energy and Material Science Research Center, Istituto Guido Donegani, Eni S.p.A., Via Fauser 4, I-28100, Novara, Italy*

† Electronic supplementary information (ESI) available: Synthetic procedures, average values for cells measurements, notes on the calibration of the indoor light source, *J*/*V* curves of different sets of cells, EIS plots, and ^{1}H and ^{13}C NMR spectra. See DOI: https://doi.org/10.1039/d3se00949a

friendly solvents would provide a clear advantage for indoor applications.

At the beginning of the century, novel environmentally responsible fluids known as deep eutectic solvents (DESs) were recognized as promising alternatives to traditional VOCs in several fields of science, such as organic synthesis,[25,26] catalysis,[27–29] main group chemistry,[30–32] materials chemistry,[33,34] extraction and separation,[35–37] crystallography,[38] and also solar technology to stabilize and improve the photovoltaic performance of DSSCs,[39–47] due to their low volatility, high thermal stability, nonflammability, ease of preparation, low cost, and tunability of their physicochemical properties. Despite these advantages, however, there are still concerns about their toxicity. Thus, new guidelines have recently been released for DES toxicity monitoring, wherever necessary.[48] DESs are generally obtained by mixing in a well-defined stoichiometric proportion, and heating, two or three safe and inexpensive components (*e.g.*, Brønsted or Lewis acids and bases, anionic and/or cationic species) that are able to form eutectic mixtures with melting points much lower than those of ideal liquid mixtures.[49,50]

As for solar technology, the use of these alternative green solvents has relied so far on typical iodide sources for the electrolyte redox pair, for instance, organic ionic liquids (*e.g.*, 1-methyl-3-propylimidazolium iodide, PMII), which are generally expensive and toxic. An eco-friendlier iodide source would be represented by inorganic iodide salts, such as KI. However, these salts are only soluble in water-based media, and they do not usually offer good performances.[51] In this work, we present a study on DES-like mixture based DSSCs where, for the first time, the electrolyte solvent itself is the sole iodide source, and I_2 is the only present component in addition to the solvent. While this paper was in preparation, H. Cruz *et al.* demonstrated that it is indeed possible to use alkali iodide-based DESs as electrolytes for DSSCs, with the best cell showing a PCE of up to 2.3%.[52]

By exploiting our expertise in DES-DSSCs,[43–45] we investigated an unprecedented DES-like mixture composed of ethylene glycol (EG) and choline iodide (ChI), which was used in place of the conventional choline chloride (ChCl). The combination of a quaternary ammonium salt (generally choline) with a hydrogen bond donor (HBD) (*e.g.*, glycerol, urea, ethylene glycol, and a carboxylic acid) is now categorized as a type III eutectic solvent.[53–55] Herein, we demonstrate that it is no longer necessary to add an external iodide source (*e.g.*, PMII) in order to form the redox couple, thereby opening the route to a new generation of DSSC devices. By properly designing the dye-sensitizer and through modulating the nature (hydrophilic *vs.* hydrophobic) of the sensitized surface of the SC, we have been able to affect the interface interaction between the SC and the electrolyte, which is particularly important in a context (such the one depicted in this manuscript) where the redox component and the solvent are the same molecule. In addition, we have shown that DSSCs sensitized by a dye, with a hydrophobic side-chain properly positioned along the molecular backbone, are able to access very high efficiencies, not only amongst the highest ever reported for DES-DSSCs, but also for water-based DSSCs. Potential indoor applications have been discussed as well.

Experimental

General information

The following materials were purchased from commercial suppliers: FTO-coated glass plates (2.2 mm thick; sheet resistance ~7 ohm per square; Solaronix); Dyesol 18NR-T transparent TiO_2 blend of active 20 nm anatase particles. UV–O_3 treatment was performed using a Novascan PSD Pro Series – digital UV–ozone system. The thickness of the layers was measured by means of a VEECO Dektak 8 Stylus Profiler. ATR FT-IR spectra were recorded with a Thermo Scientific Nicolet iS20 spectrometer.

DES-like mixture preparation

A deep eutectic solvent like mixture [choline iodide (ChI)/ethylene glycol (EG) (1 : 2 mol mol^{-1}) and choline chloride (ChCl)/EG (1 : 2 mol mol^{-1})] were prepared by heating under stirring the corresponding individual components at 60–80 °C for 10–50 min until a clear solution was obtained.

DSSC fabrication procedure

DSSCs have been prepared by adapting a procedure reported in the literature.[56] In order to exclude metal contamination, all of the containers were glass or Teflon and were treated with EtOH and 10% HCl prior to use. Plastic spatulas and tweezers have been used throughout the procedure. FTO glass plates were cleaned in a detergent solution for 15 min using an ultrasonic bath, rinsed with pure water and cleaned again for 15 min in an ultrasonic bath with EtOH. After treatment in a UV–O_3 system for 18 min, the FTO plates were treated with a freshly prepared 40 mM aqueous solution of $TiCl_4$ for 30 min at 70 °C, rinsed with water and EtOH and heated at 500 °C for 30 min.

A transparent layer of 0.20 cm^2 was screen-printed using a 20 nm transparent TiO_2 paste (Dyesol 18NR-T). The coated transparent film was dried at 125 °C for 5 min. The coated films were thermally treated at 125 °C for 5 min, 325 °C for 10 min, 450 °C for 15 min, and 500 °C for 15 min. The heating ramp rate was 5–10 °C min^{-1}. The sintered layer was treated again with 40 mM aqueous $TiCl_4$ (70 °C for 30 min), rinsed with EtOH and heated at 500 °C for 30 min. After cooling down to 80 °C, the TiO_2 coated plate was immersed in a 0.2 mM solution of the dye in the presence of the co-adsorbent (typically 1 : 10 chenodeoxycholic acid) for 20 h at room temperature in the dark.

Platinum-based counter electrodes were prepared according to the following procedure: a 1 mm hole was made in a FTO plate, using diamond drill bits. The electrodes were then cleaned with a detergent solution for 15 min using an ultrasonic bath, 10% HCl, and finally acetone for 15 min using an ultrasonic bath. Then, 10 μL of a 5×10^{-3} M solution of H_2PtCl_6 in EtOH was deposited on each electrode and the electrodes were thermally treated at 500 °C for 30 min.

The dye-adsorbed TiO_2 electrode and the counter electrode were assembled into a sealed sandwich-type cell by heating with

hot-melt ionomer-class resin (Surlyn 30 μm thickness) as a spacer between the electrodes. The same configuration was used for symmetrical dummy cells consisting of two identical dark counter electrodes working, respectively, as the anode and cathode.

The electrolyte solution was prepared by mixing at room temperature 20 mM I_2 and 2 M PMII (solutions 1 and 3) or 20 mM I_2 alone (solutions 2 and 4) in ChCl/EG or a ChI/EG 1 : 2 DES-like mixture, and kept in the dark in air. A drop of the electrolyte solution was placed over the hole and introduced inside the cell by vacuum backfilling. Finally, the hole was sealed with a sheet of Surlyn and a cover glass. A reflective foil at the backside of the counter electrode was taped to reflect unabsorbed light back to the photoanode.

DSSC measurements

PV measurements of DSSCs were carried out under a 550 W xenon light source (ABET Technologies Sun 2000 class ABA Solar Simulator). The power of the simulated light was calibrated to AM 1.5G (100 mW cm^{-2}) using a reference Si cell photodiode equipped with an IR-cutoff filter (KG-5, Schott) to reduce the mismatch in the region of 350–750 nm between the simulated light and the AM 1.5G spectrum. Indoor-light curves were obtained using a cold light T5 fluorescent lamp (Osram L 8 W/765) as the light source placed at a distance such as to illuminate the surface of interest with an illuminance equal to 1200 ± 50 lux. Illuminance was measured by using a lux meter (HoldPeak HP-881E, accuracy ±4%) for a fast check during DSSC testing, and then carefully determined from the irradiance spectrum. It is emphasized that the lux meter was only used for a rough estimation of the illuminance level and not to calculate accurate PCE, in contrast with many reports in the literature. In this work PCE was correctly determined by illuminance levels from the irradiance spectra. The emission spectrum of the light source in the wavelength range from 300 to 1000 nm was measured by using a Hamamatsu C10082CAH spectrophotometer and a power meter (Thorlabs PM100USB power and energy meter) equipped with a photodiode just calibrated for the purpose (Si-photodiode S120VC, recalibrated 03/23 by ReRa Solutions). Fig. S1† shows the spectral distribution of the irradiance (power per unit illuminated area at the distance of interest). The entire active photovoltaic area of the devices was used during indoor characterization to mimic diffuse light conditions.

In both cases, *I*/*V* curves were obtained by applying an external bias to the cell and measuring the generated photocurrent with a Keithley model 2440 digital source meter. For each combination of dye/electrolyte, multiple cells have been prepared and tested for average values of 3 independent cells. Values, including standard errors, are presented in Table S1 (see the ESI).† Incident photon-to-current conversion efficiencies (IPCEs) were recorded as a function of excitation wavelength by using a monochromator (Omni 300 LOT ORIEL) with a single grating in Czerny–Turner optical design, in AC mode with a chopping frequency of 1 Hz. EIS spectra were obtained using a Bio-logic SP-240 galvanostat potentiostat. The measurements have been performed in the frequency range from 100 kHz to 0.1 Hz under AC stimulus with 10 mV amplitude, under dark conditions or 0.23 sun solar irradiation at the open circuit voltage.[51,57] The obtained Nyquist plots have been fitted *via* a non-linear least-squares procedure using the equivalent circuit model depicted in the inset of the plot itself.

Electrochemical properties of the electrolyte solutions were investigated in thin layer (thickness of *ca.* 30 μm) dummy cells with an active area of 0.5 cm^2 by cyclic voltammetry (CV) at 10 mV s^{-1} and by electrochemical impedance spectroscopy (EIS), using the same conditions used for DSSCs, at the equilibrium potential (0 V).

Results and discussion

DSSCs based on a ChI/EG (1 : 2 mol mol^{-1}) eutectic mixture have been prepared and their photovoltaic properties were characterized. The corresponding choline chloride-based eutectic mixture presents a higher conductivity (7.63 *vs.* 0.98 mS cm^{-1}) and a lower viscosity (48 *vs.* 281 cP) compared to ChCl/glycerol (Gly) 1 : 2 (mol mol^{-1}) that we tested in our previous studies,[40,42] so we moved to EG as the HBD.[50] ChI/EG-based DESs are already present in the literature for different applications.[58,59] The eco-friendly properties of these mixtures mainly reside in their easy preparation, recyclability, low volatility, and stability in handling and storage. Of course, a more in-depth analysis on some aspects related, *e.g.*, to toxicity, biodegradability, renewable sourcing and production, should always been conducted to assess the sustainability of (new) DESs or DES-like mixtures, as has been recently pointed out in a review by Nejrotti, Bonomo and co-workers.[60]

As the used molar ratios[58,59] are different from the current value employed in this work (1 : 2), we have decided to investigate the newly formed 1 : 2 ChI/EG mixture using FT-IR and NMR spectroscopy, two techniques commonly used to study the possible intermolecular interactions taking place among components of a mixture.[61–64]

FT-IR spectra of pure components and of the 1 : 2 ChI/EG mixture are depicted in Fig. S2 (ESI).† Looking at the O–H stretching vibration region (3700–3100 cm^{-1}), the wavenumber shift of the peak of the mixture to different (higher) energies with respect to that of both the parent molecules is consistent with a different strength of the intermolecular H-bond, as a consequence of the DES formation in place of H-bond intermolecular interactions amongst the same molecular species.[61,63] Upon deconvoluting the large O–H peak of the mixture, different types of O–H contributions could be identified (Fig. 1). The deconvoluted peaks at 3545, 3423, and 3250 cm^{-1} were assigned to the O–H stretching values of the free OH group (3545)[65] and the OH-bonded groups (3423 and 3250), respectively. Based on the integration of these peaks, we can conclude that the majority of the OH groups in the mixture are involved in intermolecular hydrogen bonding interactions.[61]

To further confirm the occurrence of these interactions between the components of the 1 : 2 ChI/EG mixture, we obtained additional ^{1}H-NMR spectra, and the results are collected in Fig. S3.† The most striking difference amongst the three

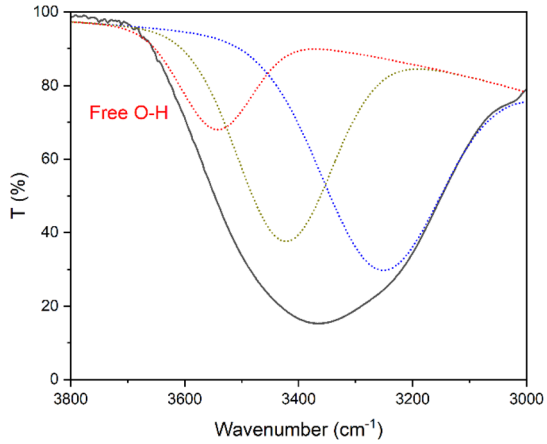

Fig. 1 FT-IR O–H stretching vibration peak deconvolution for the studied 1 : 2 ChI/EG mixture.

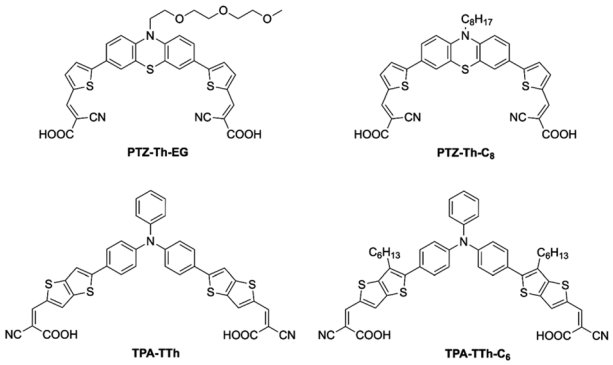

Fig. 2 Structure of the investigated dyes.

spectra was a significant broadening of the two OH resonances in the 1 : 2 ChI/EG mixture (C) in between the ranges of 5.24–5.26 and 4.42–4.45 ppm related to the OH group resonances of ChI and EG, respectively. Conversely, ^{1}H NMR spectra of ChI (A) and EG (B) present a well-resolved triplet (δ 5.20–5.24 ppm) and multiplet (4.43–4.46 ppm) for the OH signals, respectively. A slightly detectable shift was also observed between the OH signals of the 1 : 2 ChI/EG mixture (C) and ChI (A) and EG (B) with a chemical shift variation ($\Delta\delta$) of 0.04 and −0.01 ppm, respectively, in agreement with previously reported examples.[61] Such evidence suggests that the OH resonances of both ChI and EG are mutually influenced by each other, upon developing hydrogen bonding interactions between neighbouring molecules.[61,64] Although these results support the formation of a hydrogen bonding network between the two components of the used mixture, more targeted experiments would be necessary to prove that this is a real eutectic mixture. As this is outside the aim of this work, we will use, throughout the manuscript, the expression "DES-like mixture".

As for dye-sensitizers, we have first selected the same di-branched molecules previously used in our studies,[40–42] so as to better evaluate the effect of the new iodide-based DES-like mixture. In particular, two different donor–acceptor dyes based on a phenothiazine (PTZ) donor core were tested: one hydrophilic carrying a tri-ethylene glycol terminal chain (**PTZ-Th-EG**) and one hydrophobic with an *n*-C_8 alkyl terminal chain (**PTZ-Th-C_8**) (Fig. 2). In these dyes, the terminal chain is positioned on the terminal phenothiazine nitrogen atom. In the present study, we have introduced two further dyes, **TPA-TTh**[66] and **TPA-TTh-C_6**,[67] that we have previously reported in conventional VOC (acetonitrile/valeronitrile 85 : 15)-based DSSCs. These two dyes present similar absorption spectra to **PTZ-Th-EG** and **PTZ-Th-C_8**, but are based on a different chemical structure. The **TPA-TTh** and **TPA-TTh-C_6** dyes carry a commonly used triphenylamine (TPA)[7] donor core and thieno[3,2-*b*]thiophene (TTh) as a spacer, previously reported in efficient DSSC sensitizers.[66] The two dyes **TPA-TTh** and **TPA-TTh-C_6** differ only in the presence of an *n*-hexyl side-chain on the thienyl-based spacers. In contrast to the PTZ dyes, where the alkyl functionality is positioned on the terminal donor moiety, in **TPA-TTh-C_6** the alkyl groups are located on the central spacer moiety. In this way, the absence of an alkyl chain on the donor moiety should reduce the steric hindrance to dye regeneration, involving the donor group where the HOMO is located, while maintaining a side-chain barrier to minimize the detrimental charge recombination from the SC to the electrolyte.[68] All the four investigated dyes comprised conventional cyanoacrylic acids as double acceptor-anchoring points.

Four DES-like-based electrolyte compositions, listed in Table 1, have been investigated. The electrolytes differ in DES (ChCl/EG *vs.* ChI/EG) and in the presence of the commonly used PMII as a conventional iodide source. Solutions 2 and 4, based on ChCl/EG and ChI/EG, respectively, contain only iodine as an electrolyte component and not PMII. These two electrolytes are therefore "iodide-free" as they lack an external iodide source, in contrast to what is commonly reported for DSSC devices. It is worth noting that the solubility of iodine in solutions 2 and 4 was remarkably different. Only a very small quantity of I_2 could be dissolved in solution 2, which thus appeared pale-yellow coloured, whereas iodine is promptly dissolved in solution 4, thanks to the presence of the DES component ChI. The colour of solution 4 is orange-red, as expected for I^-/I_3^- mixtures. A picture of DES-like mixture solutions is presented in Fig. S4.†

To compare the four electrolytes, we started investigating their electrochemical behaviour inside dummy cells, using both CV and EIS techniques. The CV curves show a clear difference in terms of limiting current among the 4 solutions, as depicted in Fig. 3. In particular, Sol. 2 has an almost-zero limiting current together with a low slope of the curve near zero potential, accounting for a high differential resistance. Sol. 1 has a higher

Table 1 DES-like-based electrolyte compositions

DES-like solution	External iodide source	I_2	DES
1	2 M PMII	20 mM	ChCl/EG (1 : 2)
2	—	20 mM	ChCl/EG (1 : 2)
3	2 M PMII	20 mM	ChI/EG (1 : 2)
4	—	20 mM	ChI/EG (1 : 2)

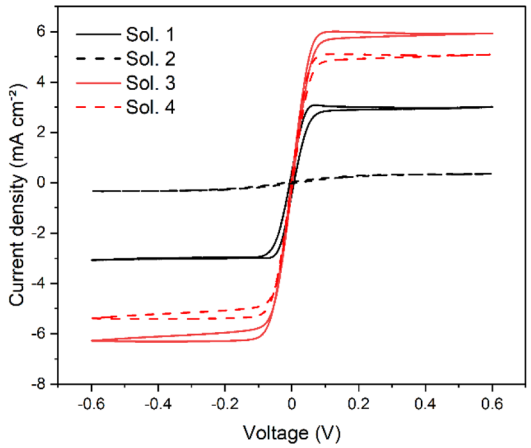

Fig. 3 CV curves of symmetrical dummy cells containing the four DES-like-based electrolyte solutions. Scan rate: 10 mV s^{-1}.

limiting current, while Sol. 3 and 4 are the best performing solutions, achieving comparable current values.

EIS investigation of the 4 dummy cells confirmed the trend obtained from CV measurements. As expected, Sol. 2 showed a highly resistive behaviour, so its curve cannot be compared to those of the other solutions (see Fig. S5†). Fig. 4 depicts Nyquist plots of Sol. 1, 3 and 4, together with the equivalent circuit used for fitting the data. R_1 accounts for the ohmic resistance of the electrolyte and of the transparent conductive oxide while the parallel resistance–capacitance (RC) circuit represents the electrochemical interface having a charge-transfer resistance in parallel with a capacitor (R_2 and C_2). The short Warburg element (W_{d3}) accounts for the diffusional impedance (Nernst impedance) of the electrolyte in the dummy cell.[69] In general, all the dummy cells exhibited common impedance features characterized by a major low-frequency loop which can be ascribed to diffusional processes, while the high-frequency loop can be ascribed to charge transfer processes, with resistance R_2. The resistance values obtained from fitting the Nyquist curves are reported in Table 2. While the charge transfer resistance is similar for all the samples (around 1 Ω), there is a clear difference in the diffusion resistance between ChCl-based solution (Sol. 1) and ChI-based solutions (Sol. 3 and 4), the first having

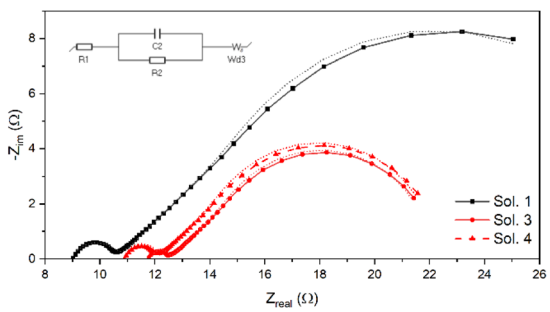

Fig. 4 Nyquist plots of dummy cells containing Sol. 1, 3 and 4. Dotted lines represent the result of the fitting with the equivalent circuit of the dummy cell (inset).

Table 2 Charge transfer resistance and diffusion resistance from Nyquist plot fitting of the dummy cells

DES-like solution	R_2 (Ω)	R_d (Ω)
1	1.38 ± 0.19	19.9 ± 1.4
3	0.64 ± 0.44	9.45 ± 0.82
4	1.02 ± 0.40	10.1 ± 0.83

a doubled resistance with respect to that of the other solutions. ChI-based solutions were thus very promising both from CV and EIS investigation results. The PV properties of the three remaining electrolytes were then assessed by preparing a first set of DSSCs based on 2.5 μm-thick-transparent TiO_2 photoanodes.

By exploiting our previous experience in DES-like-based DSSCs, an optimization of the experimental parameters has been carried out starting with a hydrophilic setup, using a polyglycolic functionalized sensitizer **PTZ-Th-EG** and the corresponding co-adsorbent, glucuronic acid (**GlcA**).[40] The preliminary screening results are collected as shown in Table S2 and depicted in Fig. S6.† With this first set of experiments, we have thus demonstrated that, using a ChI DES-like mixture as a supporting electrolyte, an external iodide source is no longer necessary because all the devices performed properly with comparable parameters. Further optimization of the parameters has been carried out by varying the co-adsorbent and then the sensitizer moving from hydrophilic **GlcA** to conventional hydrophobic chenodeoxycholic acid (**CDCA**) as a co-adsorbent (Table S2 and Fig. S7†) and then replacing the **PTZ-Th-EG dye** with the analogous alkyl functionalized **PTZ-Th-C_8** (Table S3 and Fig. S8†) sensitizer. What we noticed is that a hydrophobic functionalization allowed us to improve PCE up to 3.1% in the case of the best-performing cell with DES-like-based electrolyte 3.

This result is remarkable since it represents, to the best of our knowledge,[47] the highest PCE value ever reported for a DSSC filled with a VOC-free DES-like-based electrolyte, for which the previous record PCE value was 2.5%.[40–42,44] From the comparison of solutions 1 and 3, it can be inferred that the novel ChI/EG eutectic mixture (solution 3) provides a cooperative enhancement in combination with PMII thanks to the presence of an iodide source in the mixture, as suggested by the higher photocurrent, while retaining similar PV characteristics. Finally, the cell without an external iodide component (solution 4) also showed a steep increase in the performance, with a PCE twice that of the previous set equipped with the hydrophilic dye (see the ESI†). In order to check if the highest performance of solution 3 cells could arise from a higher iodide concentration, we have investigated a control set of DSSCs based on the conventional ChCl/EG 1 : 2 (mol mol^{-1}) DES as a solvent with different PMII concentrations. The results are reported in Table S4† and the J/V curves are depicted in Fig. S9.† We conclude that the different performances of the cells shown in Table S4† were not simply related to the different iodide concentrations in the electrolyte solutions. Thus, the use of the unconventional ChI/

EG mixture clearly provides a boosting effect on the overall performance of the cells.

The results pertaining to the devices containing the iodide-based DES-like mixture are highly encouraging, in particular when using a hydrophobic dye as a sensitizer. It is reasonable to think that the choice of a more appropriately designed hydrophobic dye could result in even higher performances. We have thus added to the study the two TPA dyes **TPA-TTh** and **TPA-TTh-C$_6$** previously introduced (Fig. 2). Since these dyes present optical properties similar to those of **PTZ-Th-C$_8$** (Fig. S10†), a comparison of the cells sensitized by **TPA-TTh-C$_6$** and **PTZ-Th-C$_8$** could allow us to evaluate the effect of inserting alkyl side chains on different parts of the sensitizer structure, namely, the spacer *vs.* donor group, respectively. In the case of **TPA-TTh-C$_6$**, the additional presence of side alkyl chains on the π-spacer should ensure a lipophilic barrier to charge recombination, while keeping the donor core of the sensitizer free from hindrance so as to optimize the dye regeneration from the electrolyte. The cells sensitized by **TPA-TTh** and **TPA-TTh-C$_6$** were thus prepared and filled with solutions 1, 3 and 4, and the corresponding results are summarized in Table S1† for **TPA-TTh** and Table 3 for **TPA-TTh-C$_6$**. The corresponding *J*/*V* curves are depicted in Fig. S11† and 5, respectively.

The two dyes presented similar efficiencies when tested in solution 1 and 3 cells. In contrast, for solution 4, that is in the absence of PMII as an external iodide source, **TPA-TTh-C$_6$** afforded a remarkably strong efficiency, with a PCE value of nearly 4%, which is much higher than that recorded with the dye without the hexyl side chains. Such a very high efficiency, which outperforms even the record value presented in Table S3,† originates from an increase in the photovoltage (up to *ca.* 0.7 V), much higher than that of any other device here investigated. This result suggests that C$_6$-alkyl chains effectively protect the TiO$_2$ surface from charge recombination in the presence of ChI as the only iodide source, while being less effective in the presence of PMII. A possible rationale could be that PMII acts as a kind of surfactant, at least partially bypassing the hydrophobic barrier provided by the dye, while letting the charged species reach the SC, thereby allowing the charge recombination. Overall, the very high efficiency recorded for the ChI-based DES-like mixture, in the absence of any external iodide source, is not only the highest observed in our work, but is even amongst the highest ever reported for VOC-free DSSCs in the presence of DES[47] or water as an unconventional green electrolyte medium and I^-/I_3^- as the redox couple.[10,13,15] It is noteworthy that the highest photocurrent obtained is almost 30% larger than the limiting current measured in the dummy

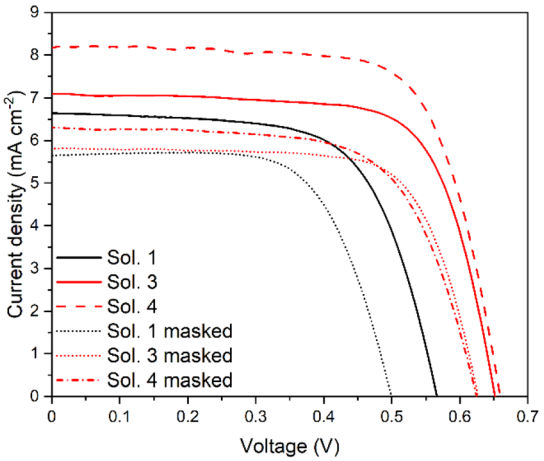

Fig. 5 *J*/*V* curves of DSSCs with ChCl *vs.* ChI DESs with **TPA-TTh-C$_6$** as the sensitizer with 1 : 10 **CDCA** as a co-adsorbent under AM1.5G, 1 sun conditions.

cells reported in Fig. 3. Nonetheless, the solar cells were measured on the temperature-controlled test stage of the solar simulator (ABET technologies) at a constant temperature of 25.0 ± 0.1 °C while diffusion-limited current in the symmetric dummy cells was recorded at room temperature (*ca.* 19 ± 1 °C). To clarify the role of the temperature, the diffusion-limited current of solution 4 was measured at different temperatures from 20 to 40 °C on the temperature-controlled test stage of the solar simulator and the results are depicted in Fig. S12.† The resulting diffusion-limited current at 25 °C is now within 15% compared to that obtained in the solar cell. A similar phenomenon has been previously observed by Bonomo and co-workers,[70] and the only possible explanation could be related to the different thicknesses of the electrolyte chamber and so a reduced diffusion pathway (see below). For comparison, we also prepared a cell using a standard VOC as the solvent, namely acetonitrile, with the same components of Sol. 1 and 3 (PMII 2 M, I_2 20 mM), resulting in a lower efficiency (2.8%) (see Fig. S13†). The same dye was also tested in an optimized cell for VOC-based electrolyte solutions (10 μm + 5 μm transparent + scattering TiO$_2$ layer, Z960 electrolyte solution[71]), yielding a 6% efficiency.

In order to better elucidate charge-recombination phenomena occurring in **TPA-TTh-C$_6$** sensitized cells, EIS measurements were performed both in the dark and under mild illumination (0.23 sun AM1.5G). In this experiment, a small sinusoidal voltage stimulus of a fixed frequency is applied to the

Table 3 Photovoltaic characteristics of a DSSC using **TPA-TTh-C$_6$** as the sensitizer and **CDCA** (10 **CDCA** : 1 dye) as a co-adsorbent[a]

DES-like solution	J_{sc} (mA cm^{-2})	V_{oc} (mV)	FF	PCE (%)	Integrated J_{sc} (mA cm^{-2})	AVT (%)	LUE (%)
1	6.6 (5.6)	566 (499)	65 (67)	2.4 (1.9)	5.3	47.7	1.2 (0.9)
3	7.1 (5.8)	652 (627)	71 (71)	3.3 (2.6)	5.6	44.4	1.5 (1.2)
4	8.2 (6.3)	661 (624)	71 (66)	3.8 (2.6)	6.0	50.7	1.9 (1.3)

[a] I_2 concentration: 0.02 M; transparent TiO$_2$ thickness: 2.5 μm. Values obtained with a 0.28 cm^2 black mask on top are in brackets.

device at the V_{oc} potential, simultaneously measuring the current response. The behaviour of the electrochemical system can be studied by varying the frequency over several orders of magnitude (generally from a few mHz to several MHz). The analysis of the impedance spectra can be performed in terms of Nyquist plots, where the imaginary part of the impedance is plotted as a function of the real part of the range of frequencies. Under dark conditions, at open-circuit voltage potential, the properties of the sensitized TiO_2/electrolyte interface can be derived by fitting the Nyquist plot with an appropriate equivalent circuit, obtaining the values of recombination resistance (R_{rec}) and chemical capacitance (C_{μ}). It is then possible to calculate the electron lifetime τ_n as $\tau_n = R_{rec} \times C_{\mu}$.[66,72] When operating under illumination it is possible to also estimate other parameters, such as the resistance associated with the diffusion in the electrolyte that could help to explain the behaviour of the cells. The parameters resulting from fitting the data obtained in the dark are listed in Table S6† and the corresponding Nyquist plot is shown in Fig. S14.† Relevant data obtained by fitting the curve under illumination are reported in Table 4 and the Nyquist plots are depicted in Fig. 6, whereas the other fitting parameters (both in the dark and under illumination) are reported in Table S7.†

Considering the data obtained by the fit of the dark EIS, it is possible to notice that the trend in V_{oc} moves the same way as the recombination resistance and the lifetime. Nonetheless, when under illumination, the cells showed very similar behaviours in terms of R_{rec}, but a large difference is evidenced in the diffusion resistance, and thus in the transport losses, which could be the explanation for the very different performances of the cells.[52] In particular, these results match the R_d trend measured in dummy cells pretty well, with Sol. 4 showing half the resistance of Sol. 1, while Sol. 3 seems to have a higher diffusion resistance in the full cell than in the dummy cell, which is however lower than that of Sol. 1.

Finally, we also evaluated the incident photon-to-current efficiency (IPCE) of DSSCs sensitized with **TPA-TTh-C$_6$**, and the curves are shown in Fig. 7. For all the investigated devices, IPCE curves resemble the UV-vis absorption spectrum of **TPA-TTh-C$_6$** shifted towards lower energies (Fig. 7 and S10,† green line). The shape of the curves is similar in the three different electrolyte solutions, with a wide absorption up to *ca.* 600 nm and a maximum at *ca.* 490 nm. The trend of IPCE curves is consistent with the performance of the cells. In particular, the highest IPCE value has been recorded for the cell filled with solution 4, with a remarkable peak of *ca.* 86%. Moreover, the integrated photocurrent calculated from the IPCE spectra well matches the value recorded for the corresponding cells measured under AM1.5G conditions with a black mask on top reported in Table 3.

Another important parameter that could be considered when dealing with transparent devices that could be integrated into buildings, automotives or other see-through applications is the impact of the colour of the final device on the visual perception of human eyes. It is possible to also evaluate the efficiency of the cells with respect to this parameter. To estimate the impact of the device transparency, the average visible transmittance (AVT) could be calculated considering the transmittance spectrum, the photopic response of human eyes and the photon flux of the solar spectrum under AM1.5G conditions.[73] Fig. 8 depicts the total transmission spectra of the complete devices sensitized with **TPA-TTh-C$_6$** using the three different electrolytes investigated in this work. It can be noted that the absorption of the sensitizer is mainly located in the high energy region of the visible spectrum (below 550 nm, see Fig. S10†) poorly influencing the perception of the colour by the human eyes. A small difference could be seen in the device using Sol. 3 where the content of iodide is larger and a lower transmittance in the corresponding region is observed. The calculated AVT value ranges from about 44 to 51% for the best cell which is a remarkable value considering that these are non-wavelength-selective devices. Considering the device efficiency, starting

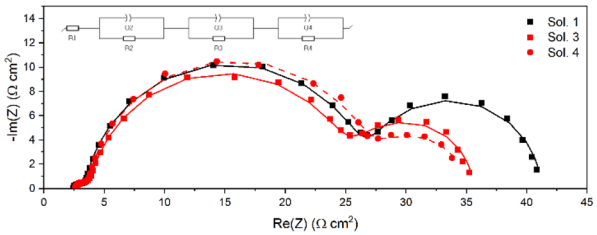

Fig. 6 EIS data plots of DSSCs under illumination (0.23 sun) as described in Table 4. Lines represent the result of the fitting with the equivalent circuit in the inset.

Table 4 Recombination and diffusion resistance obtained from Nyquist plot data fitting of a DSSC using **TPA-TTh-C$_6$** as the sensitizer and **CDCA** (10 **CDCA** : 1 dye) as a co-adsorbent under 0.23 sun irradiation

DES solution	R_{rec} (Ω cm^2)	R_{diff} (Ω cm^2)
1	23.44 ± 0.14	14.39 ± 0.16
3	21.66 ± 0.20	10.08 ± 0.20
4	23.91 ± 0.24	7.39 ± 0.31

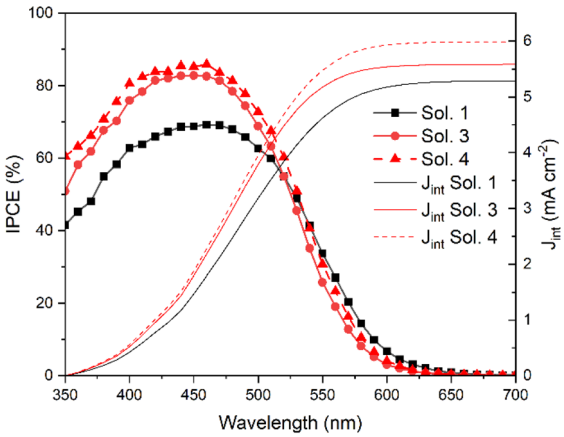

Fig. 7 IPCE curves of **TPA-Th-C$_6$** sensitized cells. Dashed: integrated photocurrent from IPCE spectra ofthe solar cell.

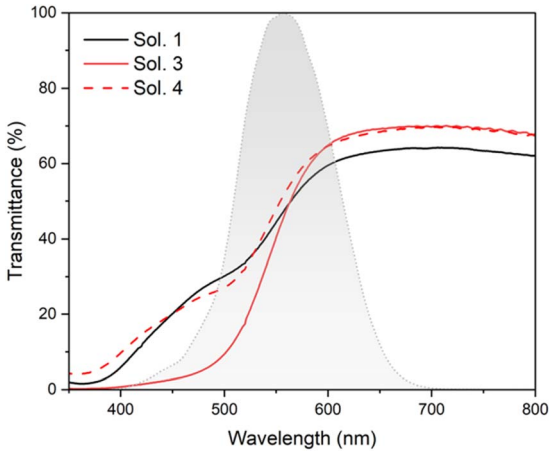

Fig. 8 Comparison of the cell transmittance with different electrolyte solutions. The human eye photopic response is included for comparison with the eye's sensitivity.

from the AVT, it is possible to calculate the light utilization efficiency (LUE) as the product of cell efficiency and AVT.[73,74] This parameter could provide a reasonable parameter to compare the performances of different transparent devices. Values of AVT and LUE of the investigated devices are reported in Table 3.

Stability testing

Short- and mid-term temporal stability of PV parameters of DES-like based DSSCs was tested over a period of 1, 3, 7, 45, and 70 days. During this time the cells were stored in the dark. In particular, we have compared stability data of cells sensitized by the two representative dyes of this work, **PTZ-Th-C$_8$** and **TPA-TTh-C$_6$**, both in ChCl and ChI-based electrolyte solvents. The results are depicted in Fig. 9.

It shows that **TPA-TTh-C$_6$** devices were in general much more stable than **PTZ-Th-C$_8$** cells and, at the same time, the presence of the ChI/EG DES-like mixture improved the temporal stability compared to the conventional ChCl/EG counterpart. In particular, **PTZ-Th-C$_8$** sensitized cells filled with solution 1 lost almost 70% of the initial efficiency after 10 days. **PTZ-Th-C$_8$** sensitized devices filled with ChI/EG still retained more than 60% of the starting value even after 70 days (cells with solutions 3 and 4 were less efficient by 40 and 32%, respectively). Temporal stabilities were significantly improved when using **TPA-TTh-C$_6$** as a sensitizer. Cells filled with solution 1 (ChCl/EG) still retained 60% of the starting efficiency at the end of the 70-day testing period. The corresponding devices filled with solutions 3 and 4, based on the ChI/EG DES-like mixture, retained 88 and 93% of the initial efficiency, respectively.

It is also interesting to note that the efficiency of cells sensitized by **TPA-TTh-C$_6$** showed a slight increase in PCE in the first few days, in particular when filled with the ChI/EG DES-like mixture, reaching a maximum of 3.86% with solution 4 on day 4. This behaviour could be ascribed to a slow permeation of the electrolyte solution into the sensitized layer, which may require

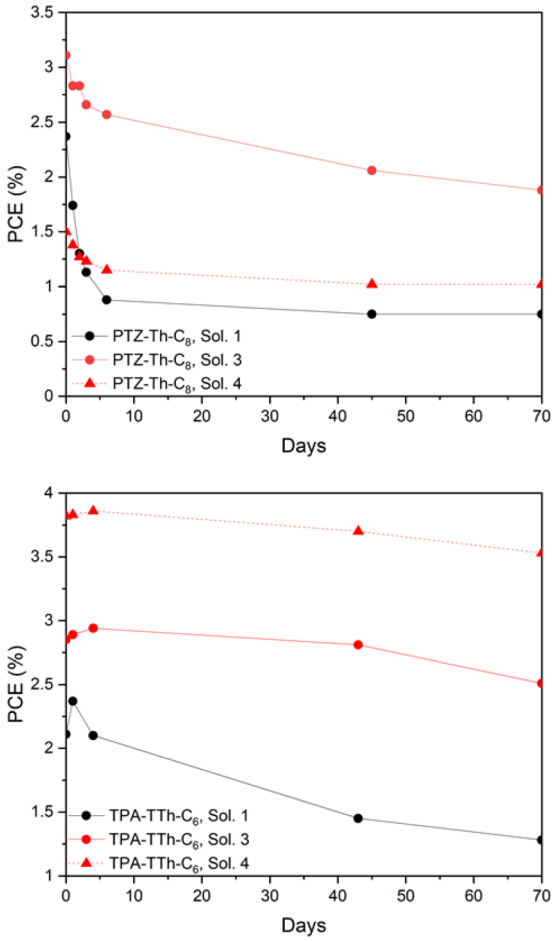

Fig. 9 PCE of **PTZ-Th-C$_8$** (top) and **TPA-TTh-C$_6$** (bottom) sensitized DSSCs in combination with **CDCA** as a co-adsorbent, filled with solutions 1, 3 and 4 (recordings up to 70 days from the initial cell assembly) recorded under AM1.5G irradiation.

some time to pass through the hydrophobic barrier exerted by the dye.

On the whole, the stability results are remarkable since they clearly show that an appropriate combination of a specifically designed dye (TPA-based with an alkyl chain on the spacer unit) and DES-like mixture as the active electrolyte solvent (ChI/EG) affords devices with basically full stability (7% decrease) over a period of more than 2 months. This result is even more attractive if compared to previously reported stability data in the literature on DES-DSSCs. Cruz and co-workers recently reported that an N719-sensitized DSSC filled with alkali-iodide-based DESs presented a 50% loss of efficiency after 1 month.[52] It is worth noting that also, in their case, the stability of DES-like based cells was higher than the stability of those filled with VOC-based solvents.

PV measurements under low light illumination (indoor light environment)

Lastly, we have tested the DES-like based DSSCs investigated in this work under low light illumination, that is under simulated indoor light conditions. To the best of our knowledge, previous

Table 5 Photovoltaic characteristics of DSSCs using **PTZ-Th-C$_8$** or **TPA-TTh-C$_6$** as sensitizers and **CDCA** (10 : 1) under 1200 lux light illumination

Dye	DES-like solution[a]	J_{sc} (μA cm^{-2})	V_{oc} (mV)	FF	PCE (%)	Max power (μW cm^{-2})
PTZ-Th-C$_8$	1	72	412	52	4.2	15.6
	3	103	434	67	8.0	29.8
	4	50	364	64	2.1	8.0
TPA-TTh-C$_6$	1	97	346	65	5.8	21.6
	3	89	384	71	6.5	24.3
	4	79	523	72	8.0	29.5

[a] I_2 concentration: 0.02 M; transparent TiO_2 thickness: 2.5 μm.

literature reports only one example of a VOC-free environmentally friendly water-based DSSC for indoor applications, with the best cell showing a PCE value of 7.2% at 1000 lux.[75] Cells sensitized by **PTZ-Th-C$_8$** and **TPA-TTh-C$_6$** dyes were tested, in the presence of ChCl/EG and ChI/EG DES-based electrolytes, under a 1200-lux 6400 K T5 fluorescent tube (measured emission power of 3.71 W m^{-2}). This illumination is the one typically observed in common indoor environments, such as supermarkets, offices, or hotel lounges.

We have taken particular care in measuring the power of the light source since, with the increasing interest in indoor PV applications, many questions related to the reliability of the published efficiencies have been raised.[76–78] In fact, common commercially available lux meters are somewhat inaccurate for measuring the illuminance of LEDs or fluorescent lamps and cannot be used to calculate the irradiance. In contrast, knowing the real irradiance spectrum of the lamp makes it possible to precisely calculate the lux emitted by the light source.[76,78] For this reason, we developed an easy way to reliably quantify the correct irradiance of the lamp using just a calibrated Si-photodiode and the emission spectrum of the light source recorded by using a spectrometer, from which we then calculated the lux (see the ESI† for all the details). As a comparison, the value of 1200 lux measured by this rigorous method is equivalent to *ca.* 1000 lux measured with common commercially available lux meters. In this manner, and we believe, in many reports in the literature, the measured PCE would have been overestimated.

The resulting PV parameters are collected and shown in Table 5 and the corresponding *J*/*V* curves are depicted in Fig. S15 and S16.†

Generated photocurrent densities are much lower than those under 1 sun illumination, as expected from the low incident photon flux. Cells based on the ChI/EG DES-like mixture showed higher FF values than cells containing ChCl/EG. In particular, **PTZ-Th-C$_8$** sensitized cells filled with solution 3 and **PTZ-TTh-C$_6$** sensitized cells filled with solution 4 offered the best performance, with PCE reaching the remarkable value of 8%. These results are just slightly lower than that of VOC-based cells with similar characteristics (similar power input, no co-sensitization, and I^-/I_3^- based electrolyte),[79] and outmatch the only example reported in the literature for VOC-free water-based DSSCs under ambient light.[75] Once again, the ChI/EG electrolyte showed superior performances compared to the ChCl/EG counterpart. Interestingly, cells sensitized with **PTZ-Th-C$_8$** also recorded a very poor efficiency in solution 4, whereas devices in the presence of **TPA-TTh-C$_6$** showed a PCE equal to or higher than 5.8% in any DES solution, thus offering a higher degree of reliability and constancy of results.

Since there is no standardized equipment for low light measurements yet, in Table 5 we have listed the maximum generated power, which is independent of light source calibration in contrast to PCE values. In addition, power values are more important for practical applications, as recently stressed by the representative literature.[80] Our best devices, that is, **PTZ-Th-C$_8$** sensitized cells filled with solution 3 and **TPA-TTh-C$_6$** sensitized cells filled with solution 4, presented power values of *ca.* 30 μW cm^{-2}, which compare well with literature values.[75,79,81] Such power quantities well match the power required by small electronic appliances,[23,82] such as TV remote controls, for a 4 cm^2 device area, and small wireless sensors.

Conclusions

In conclusion, we have herein presented an extensive study aimed at exploring the possibility of using iodide-based unconventional DES-like mixtures as active electrolyte solvents, with no external iodide sources. Such a device structure is totally novel compared to typical DSSCs so far set-up, where VOCs and external iodide sources such as PMII are routinely used.

In combination with an appropriate cell optimization (*i.e.*, choice of the co-adsorbent and SC layer thickness) and, in particular, of tailored dye design (a TPA dye with a hydrophobic chain on the median spacer unit), we have been able to achieve top-ranked PCEs for DSSCs based on a non-VOC solvent. The obtained PCE of nearly 4% is amongst the best ever reported values even for water-based DSSCs, and represents a record value for DSSCs based on DESs as the electrolyte media in the complete absence of VOCs as co-solvents. The best combination of **TPA-TTh-C$_6$** dye and ChI/EG as a DES-like mixture is also able to provide a remarkable temporal stability of nearly 95% over a period longer than 2 months. As transparent devices, the thus obtained cells showed good transparency and values of AVT comparable with those of common non-wavelength-selective devices (around 50% AVT) thus offering the possibility for different see-through applications. Lastly, we have also shown that the novel DES-like-DSSCs offer top-ranked PCEs under low

light illumination, exceeding, to the best of our knowledge, literature values based on traditional Ru-based sensitizers and environmentally friendly solvents such as water. We believe that these findings could pave the way towards a new generation of simpler, low-cost, and high performing DSSC devices, with great potential, in particular, for indoor practical applications.

Author contributions

Chiara Liliana Boldrini: investigation, validation, writing – original draft. Andrea Francesca Quivelli: investigation, validation, writing – original draft. Filippo Maria Perna: investigation, writing – review and editing. Paolo Biagini: funding acquisition, writing – review and editing. Vito Capriati: funding acquisition, writing – review and editing. Alessandro Abbotto: funding acquisition, writing – review and editing. Norberto Manfredi: conceptualization, supervision, visualization, funding acquisition, writing – review and editing.

Conflicts of interest

There are no conflicts to declare.

Acknowledgements

C. L. B., A. F. Q., A. A., and N. M. wish to thank Prof. M. Acciarri, Dipartimento di Scienza dei Materiali, Università degli Studi di Milano-Bicocca, for the fruitful discussion on measuring the power of the fluorescent lamp used for indoor characterization of DSSCs. This work was carried out under the framework of the national PRIN project "Unlocking Sustainable Technologies Through Nature-inspired Solvents" (NATUREChem) (grant number: 2017A5HXFC_004). The authors wish to acknowledge the Ministero dell'Università e della Ricerca (MUR) for financial support. Financial support from MUR (grant Dipartimenti di Eccellenza – 2017 "Materials for Energy") and University of Milano-Bicocca (Fondo di Ateneo – Quota Competitiva 2017 and 2019) is also gratefully acknowledged by C. L. B., A. F. Q., N. M., and A. A. This work was also performed under research contract no. 3500010866 between Milano-Bicocca Solar Energy Research Center – MIB-Solar, University of Milano-Bicocca and Eni S.p.A, Rome. F. M. P. and V. C. acknowledge the University of Bari and Interuniversity Consortium C.I.N.M.P.I.S. for financial support.

References

1 IRENA, *Renewable Power Generation Costs in 2020*, International Renewable Energy Agency, Abu Dhabi, 2021.
2 REN21, *Renewables Global Status Report*, Paris, 2021.
3 NREL, *Best Research-Cell Efficiencies*, 2022.
4 B. O'Regan and M. Gratzel, *Nature*, 1991, **353**, 737–740.
5 M. A. Saeed, K. Yoo, H. C. Kang, J. W. Shim and J.-J. Lee, *Dyes Pigm.*, 2021, **194**, 109626.
6 D. Devadiga, M. Selvakumar, P. Shetty and M. S. Santosh, *J. Power Sources*, 2021, **493**, 229698.
7 A. Mahmood, *Sol. Energy*, 2016, **123**, 127–144.
8 J. Wu, Z. Lan, J. Lin, M. Huang, Y. Huang, L. Fan and G. Luo, *Chem. Rev.*, 2015, **115**, 2136–2173.
9 Y. Ren, D. Zhang, J. Suo, Y. Cao, F. T. Eickemeyer, N. Vlachopoulos, S. M. Zakeeruddin, A. Hagfeldt and M. Grätzel, *Nature*, 2023, **613**, 60–65.
10 N. Mariotti, M. Bonomo, L. Fagiolari, N. Barbero, C. Gerbaldi, F. Bella and C. Barolo, *Green Chem.*, 2020, **22**, 7168–7218.
11 N. Mariotti, M. Bonomo and C. Barolo, *Reliability and Ecological Aspects of Photovoltaic Modules*, IntechOpen, Rijeka, 2020.
12 F. Bella, C. Gerbaldi, C. Barolo and M. Grätzel, *Chem. Soc. Rev.*, 2015, **44**, 3431–3473.
13 S. Galliano, F. Bella, M. Bonomo, F. Giordano, M. Grätzel, G. Viscardi, A. Hagfeldt, C. Gerbaldi and C. Barolo, *Sol. RRL*, 2021, **5**, 2000823.
14 L. Fagiolari, M. Bonomo, A. Cognetti, G. Meligrana, C. Gerbaldi, C. Barolo and F. Bella, *ChemSusChem*, 2020, **13**, 6562–6573.
15 C. Law, O. Moudam, S. Villarroya-Lidon and B. O'Regan, *J. Mater. Chem.*, 2012, **22**, 23387–23394.
16 F. Bella, L. Porcarelli, D. Mantione, C. Gerbaldi, C. Barolo, M. Grätzel and D. Mecerreyes, *Chem. Sci.*, 2020, **11**, 1485–1493.
17 D. Devadiga, M. Selvakumar, P. Shetty and M. S. Santosh, *J. Electron. Mater.*, 2021, **50**, 3187–3206.
18 D. Zhang, M. Stojanovic, Y. Ren, Y. Cao, F. T. Eickemeyer, E. Socie, N. Vlachopoulos, J.-E. Moser, S. M. Zakeeruddin, A. Hagfeldt and M. Grätzel, *Nat. Commun.*, 2021, **12**, 1777.
19 E. Tanaka, H. Michaels, M. Freitag and N. Robertson, *J. Mater. Chem. A*, 2020, **8**, 1279–1287.
20 H. Michaels, M. Rinderle, R. Freitag, I. Benesperi, T. Edvinsson, R. Socher, A. Gagliardi and M. Freitag, *Chem. Sci.*, 2020, **11**, 2895–2906.
21 A. Jagadeesh, G. Veerappan, P. S. Devi, K. N. N. Unni and S. Soman, *J. Mater. Chem. A*, 2023, **11**, 14748–14759.
22 H. Michaels, M. Rinderle, I. Benesperi, R. Freitag, A. Gagliardi and M. Freitag, *Chem. Sci.*, 2023, **14**, 5350–5360.
23 I. Mathews, S. N. Kantareddy, T. Buonassisi and I. M. Peters, *Joule*, 2019, **3**, 1415–1426.
24 K.-L. Wang, Y.-H. Zhou, Y.-H. Lou and Z.-K. Wang, *Chem. Sci.*, 2021, **12**, 11936–11954.
25 D. A. Alonso, A. Baeza, R. Chinchilla, G. Guillena, I. M. Pastor and D. J. Ramon, *Eur. J. Org Chem.*, 2016, **2016**, 612–632.
26 L. Cicco, G. Dilauro, F. M. Perna, P. Vitale and V. Capriati, *Org. Biomol. Chem.*, 2021, **19**, 2558–2577.
27 S. E. Hooshmand, R. Afshari, D. J. Ramón and R. S. Varma, *Green Chem.*, 2020, **22**, 3668–3692.
28 A. Torregrosa-Chinillach, A. Sanchez-Lao, E. Santagostino and R. Chinchilla, *Molecules*, 2019, **24**, 4058.
29 G. Dilauro, L. Cicco, P. Vitale, F. M. Perna and V. Capriati, *Eur. J. Org Chem.*, 2023, **26**, e202200814.
30 F. M. Perna, P. Vitale and V. Capriati, *Curr. Opin. Green Sustainable Chem.*, 2021, **30**, 100487.
31 G. Dilauro, C. Luccarelli, A. F. Quivelli, P. Vitale, F. M. Perna and V. Capriati, *Angew. Chem., Int. Ed.*, 2023, **62**, e202304720.

32 S. E. García-Garrido, A. Presa Soto, E. Hevia and J. García-Álvarez, *Eur. J. Inorg. Chem.*, 2021, **2021**, 3116–3130.
33 D. Carriazo, M. C. Serrano, M. C. Gutiérrez, M. L. Ferrer and F. del Monte, *Chem. Soc. Rev.*, 2012, **41**, 4996–5014.
34 F. del Monte, D. Carriazo, M. C. Serrano, M. C. Gutiérrez and M. L. Ferrer, *ChemSusChem*, 2014, **7**, 999–1009.
35 X. Li and K. H. Row, *J. Sep. Sci.*, 2016, **39**, 3505–3520.
36 L. Duan, L.-L. Dou, L. Guo, P. Li and E. H. Liu, *ACS Sustainable Chem. Eng.*, 2016, **4**, 2405–2411.
37 F. Pena-Pereira and J. Namieśnik, *ChemSusChem*, 2014, **7**, 1784–1800.
38 B. D. Belviso, F. M. Perna, B. Carrozzini, M. Trotta, V. Capriati and R. Caliandro, *ACS Sustainable Chem. Eng.*, 2021, **9**, 8435–8449.
39 H.-R. Jhong, D. S.-H. Wong, C.-C. Wan, Y.-Y. Wang and T.-C. Wei, *Electrochem. Commun.*, 2009, **11**, 209–211.
40 C. L. Boldrini, N. Manfredi, F. M. Perna, V. Trifiletti, V. Capriati and A. Abbotto, *Energy Technol.*, 2017, **5**, 345–353.
41 C. L. Boldrini, N. Manfredi, F. M. Perna, V. Capriati and A. Abbotto, *Chem.–Eur. J.*, 2018, **24**, 17656–17659.
42 C. L. Boldrini, N. Manfredi, F. M. Perna, V. Capriati and A. Abbotto, *ChemElectroChem*, 2020, **7**, 1707–1712.
43 M. Heydari Dokoohaki, F. Mohammadpour and A. R. Zolghadr, *J. Phys. Chem. C*, 2021, **125**, 15155–15165.
44 D. J. Boogaart, J. B. Essner and G. A. Baker, *J. Chem. Phys.*, 2021, **155**, 061102.
45 P. T. Nguyen, T.-D. T. Nguyen, V. S. Nguyen, D. T.-X. Dang, H. M. Le, T.-C. Wei and P. H. Tran, *J. Mol. Liq.*, 2019, **277**, 157–162.
46 D. Nguyen, T. Van Huynh, V. S. Nguyen, P.-L. Doan Cao, H. T. Nguyen, T.-C. Wei, P. H. Tran and P. T. Nguyen, *RSC Adv.*, 2021, **11**, 21560–21566.
47 C. L. Boldrini, A. F. Quivelli, N. Manfredi, V. Capriati and A. Abbotto, *Molecules*, 2022, **27**, 709.
48 J. Torregrosa-Crespo, X. Marset, G. Guillena, D. J. Ramón and R. María Martínez-Espinosa, *Sci. Total Environ.*, 2020, **704**, 135382.
49 E. L. Smith, A. P. Abbott and K. S. Ryder, *Chem. Rev.*, 2014, **114**, 11060–11082.
50 B. B. Hansen, S. Spittle, B. Chen, D. Poe, Y. Zhang, J. M. Klein, A. Horton, L. Adhikari, T. Zelovich, B. W. Doherty, B. Gurkan, E. J. Maginn, A. Ragauskas, M. Dadmun, T. A. Zawodzinski, G. A. Baker, M. E. Tuckerman, R. F. Savinell and J. R. Sangoro, *Chem. Rev.*, 2021, **121**, 1232–1285.
51 F. Bella, S. Galliano, M. Falco, G. Viscardi, C. Barolo, M. Grätzel and C. Gerbaldi, *Chem. Sci.*, 2016, **7**, 4880–4890.
52 H. Cruz, A. L. Pinto, N. Jordão, L. A. Neves and L. C. Branco, *Sustainable Chem.*, 2021, **2**, 222–236.
53 A. P. Abbott, J. C. Barron, K. S. Ryder and D. Wilson, *Chem.–Eur. J.*, 2007, **13**, 6495–6501.
54 C. Florindo, F. S. Oliveira, L. P. N. Rebelo, A. M. Fernandes and I. M. Marrucho, *ACS Sustainable Chem. Eng.*, 2014, **2**, 2416–2425.
55 B. Gurkan, H. Squire and E. Pentzer, *J. Phys. Chem. Lett.*, 2019, **10**, 7956–7964.
56 S. Ito, T. N. Murakami, P. Comte, P. Liska, C. Grätzel, M. K. Nazeeruddin and M. Grätzel, *Thin Solid Films*, 2008, **516**, 4613–4619.
57 F. Bella, S. Galliano, G. Piana, G. Giacona, G. Viscardi, M. Grätzel, C. Barolo and C. Gerbaldi, *Electrochim. Acta*, 2019, **302**, 31–37.
58 Q. Li, J. Jiang, G. Li, W. Zhao, X. Zhao and T. Mu, *Sci. China: Chem.*, 2016, **59**, 571–577.
59 M. Vagnoni, C. Samorì and P. Galletti, *J. CO2 Util.*, 2020, **42**, 101302.
60 S. Nejrotti, A. Antenucci, C. Pontremoli, L. Gontrani, N. Barbero, M. Carbone and M. Bonomo, *ACS Omega*, 2022, **7**, 47449–47461.
61 H. Wang, S. Liu, Y. Zhao, J. Wang and Z. Yu, *ACS Sustainable Chem. Eng.*, 2019, **7**, 7760–7767.
62 M. A. Sedghamiz and S. Raeissi, *J. Mol. Liq.*, 2018, **269**, 694–702.
63 L. H. Xu, D. Wu, Y. W. Zhu, X. Y. Chen and Z. J. Zhang, *J. Energy Storage*, 2022, **48**, 103955.
64 J. M. Silva, C. V. Pereira, F. Mano, E. Silva, V. I. B. Castro, I. Sá-Nogueira, R. L. Reis, A. Paiva, A. A. Matias and A. R. C. Duarte, *ACS Appl. Bio Mater.*, 2019, **2**, 4346–4355.
65 V. Crupi, G. Maisano, D. Majolino, P. Migliardo and V. Venuti, *J. Phys. Chem. A*, 2000, **104**, 3933–3939.
66 N. Manfredi, V. Trifiletti, F. Melchiorre, G. Giannotta, P. Biagini and A. Abbotto, *New J. Chem.*, 2018, **42**, 9281–9290.
67 A. Abbotto, M. F. Acciarri, P. Biagini, S. O. Binetti and S. P. A. Eni, *US Pat.*, 20150221871A1, 2015.
68 N. Koumura, Z.-S. Wang, S. Mori, M. Miyashita, E. Suzuki and K. Hara, *J. Am. Chem. Soc.*, 2008, **130**, 4202–4203.
69 A. Hauch and A. Georg, *Electrochim. Acta*, 2001, **46**, 3457–3466.
70 M. Bonomo, E. J. Ekoi, A. G. Marrani, A. Y. Segura Zarate, D. P. Dowling, C. Barolo and D. Dini, *Sustainable Energy Fuels*, 2021, **5**, 4736–4748.
71 C.-Y. Chen, M. Wang, J.-Y. Li, N. Pootrakulchote, L. Alibabaei, C.-h. Ngoc-le, J.-D. Decoppet, J.-H. Tsai, C. Grätzel, C.-G. Wu, S. M. Zakeeruddin and M. Grätzel, *ACS Nano*, 2009, **3**, 3103–3109.
72 F. Fabregat-Santiago, G. Garcia-Belmonte, I. Mora-Sero and J. Bisquert, *Phys. Chem. Chem. Phys.*, 2011, **13**, 9083–9118.
73 Z. Hu, J. Wang, X. Ma, J. Gao, C. Xu, K. Yang, Z. Wang, J. Zhang and F. Zhang, *Nano Energy*, 2020, **78**, 105376.
74 C. J. Traverse, R. Pandey, M. C. Barr and R. R. Lunt, *Nat. Energy*, 2017, **2**, 849–860.
75 M. Jilakian and T. H. Ghaddar, *ACS Appl. Energy Mater.*, 2022, **5**, 257–265.
76 D. Lübke, P. Hartnagel, J. Angona and T. Kirchartz, *Adv. Energy Mater.*, 2021, **11**, 2101474.
77 C.-Y. Chen, Z.-H. Jian, S.-H. Huang, K.-M. Lee, M.-H. Kao, C.-H. Shen, J.-M. Shieh, C.-L. Wang, C.-W. Chang, B.-Z. Lin, C.-Y. Lin, T.-K. Chang, Y. Chi, C.-Y. Chi, W.-T. Wang, Y. Tai, M.-D. Lu, Y.-L. Tung, P.-T. Chou, W.-T. Wu, T. J. Chow, P. Chen, X.-H. Luo, Y.-L. Lee, C.-C. Wu, C.-M. Chen, C.-Y. Yeh, M.-S. Fan, J.-D. Peng, K.-C. Ho, Y.-N. Liu, H.-Y. Lee, C.-Y. Chen, H.-W. Lin,

C.-T. Yen, Y.-C. Huang, C.-S. Tsao, Y.-C. Ting, T.-C. Wei and C.-G. Wu, *J. Phys. Chem. Lett.*, 2017, **8**, 1824–1830.
78 A. Venkateswararao, J. K. W. Ho, S. K. So, S.-W. Liu and K.-T. Wong, *Mater. Sci. Eng., R*, 2020, **139**, 100517.
79 C. Hora, F. Santos, M. G. F. Sales, D. Ivanou and A. M. Mendes, *ACS Appl. Energy Mater.*, 2022, **5**, 14846–14857.
80 H. Michaels, I. Benesperi and M. Freitag, *Chem. Sci.*, 2021, **12**, 5002–5015.
81 R. Haridas, J. Velore, S. C. Pradhan, A. Vindhyasarumi, K. Yoosaf, S. Soman, K. N. N. Unni and A. Ajayaghosh, *Adv. Mater.*, 2021, **2**, 7773–7787.
82 K. Soyeon, J. Muhammad, J. Jae Hoon and L. Dong Chan, *Curr. Altern. Energy*, 2019, **3**, 3–17.